POLSKA AKADEMIA NAUK

INSTYTUT MASZYN PRZEPŁYWOWYCH

TRANSACTIONS OF THE INSTITUTE OF FLUID-FLOW MACHINERY

PRACE INSTYTUTU MASZYN PRZEPŁYWOWYCH

98

WYDAWNICTWO IMP PAN

GDAŃSK 1995

PRACE INSTYTUTU MASZYN PRZEPŁYWOWYCH

poświęcone są publikacjom naukowym z zakresu teorii i badań doświadczalnych w dziedzinie mechaniki i termodynamiki przepływów, ze szczególnym uwzględnieniem problematyki maszyn przepływowych

*

THE TRANSACTIONS OF THE INSTITUTE OF FLUID-FLOW MACHINERY

exist for the publication of theoretical and experimental investigations of all aspects of the mechanics and thermodynamics of fluid-flow with special reference to fluid-flow machines

REDAKCJA – EDITORIAL OFFICE

Wydawnictwo Instytutu Maszyn Przepływowych
Polskiej Akademii Nauk
ul. Gen. Józefa Fiszera 14, 80-952 Gdańsk, skr. poczt. 621,
☎ (0-58) 46-08-81 wew. 141, fax: (0-58) 41-61-44,
e-mail: tjan@imppan.imp.pg.gda.pl

ISBN 83-01-95428-1
ISSN 0079-3205

PRACE INSTYTUTU MASZYN PRZEPŁYWOWYCH

1995 Zeszyt 98

MARIAN TRELA[1], JANUSZ RYMKIEWICZ[1], EUGENIUSZ IHNATOWICZ[1]

Investigation of radial spread of liquid stream on a horizontal plate[2]

The radial flow of a thin liquid film on a horizontal plate formed by the impingement of a circular liquid jet is studied both theoretically and experimentally. The change of film thickness has been examined for different flow zones, encompassing also the phenomenon of hydraulic jump. Results of our own experimental data of film thickness have been presented and compared against calculated values.

Nomenclature

a	– radius of oncoming jet,	R	– quantity described by Eq. (2.45),
b	– coefficient, $(= 2\gamma)$,	Re	– Reynolds number, $(= Q/\nu a)$,
C_f	– friction coefficient,	Re_h	– Reynolds number, $(= hU/\nu)$,
d	– nozzle diameter $(= 2a)$,	U	– surface velocity,
Fr	– Froude number $(= U/(gh)^{1/2})$,	u	– r-coordinate velocity component,
$\overline{Fr}$	– mean Froude number, $(= \overline{u}/\{gh\}^{1/2})$,	$\overline{u}$	– mean velocity,
$f(\eta)$	– non-dimensional velocity profile, $(= u/U)$,	w	– y-coordinate velocity component,
g	– gravity,	y	– vertical comp. in cylindrical coordinates,
h	– liquid layer thickness (film),	α, β	– coefficients in Table 1,
K_i	– quantity described by Eq. (2.11), $i = 1, 2$,	γ	– coefficient described by Eq. (2.11),
		δ	– boundary layer thickness,
l	– integration constant,	ν	– kinematic viscosity,
p	– pressure,	ρ	– density,
Q	– volumetric flow rate,	η	– non-dimensional film thickness, $(= y/h)$,
r	– radius, coordinate in cylindrical coordinates,	τ	– shear stress,
		ω, Ω	– quantity defined in the text and Table 1.

Subscripts

0	– of potential velocity, of boundary layer, film thickness,	r	– coordinate r,
		w	– wall,
m	– minimum film thickness,	$*$	– non-dimensional quantity.
p	– hydraulic jump,		

[1]Department of Thermodynamics and Heat Exchange, Institute of Fluid-Flow Machinery, ul. Fiszera 14, 80-952 Gdańsk

[2]The work was sponsored by a research project KBN No 39 404 030 06

1. Introduction

Liquid impingement jets are widely used in a variety of technical applications, for example in glass and metal industries, as an effective way of cooling surfaces. Recently, a great deal of interest is centred on intensive cooling of highly loaded electronic components. In a natural way this form of flow exists in spray cooled heat exchangers or in condensers. Liquid streams flowing down from one element onto another spread on the surface of a horizontal pipe as a liquid film. Film thickness and its range influence the intensity of heat transfer from that surface. So far, the problem of flow spread has been analysed for a horizontal surface wetted by a vertical impinging jet [1,2]. In the present work, an analysis of liquid jet spread on a horizontal surface is presented. It enables the indentification of different flow zones. Close attention has been devoted to the formation of hydraulic jump, which is unprofitable for heat transfer phenomena. Various velocity profiles in the liquid layer have been analysed in the light of their influence on the solution of flow equation. The results of our own experimental investigations of liquid film thickness are presented against the results of numerical computations in the supercritical and subcritical regions. The idea of this work is to verify existing methods of stream spread on a horizontal surface which will be very useful later in the analysis of more complex situations like jet spread on a horizontal cylinder. Particular attention has been paid to the calculation of film thickness in the subcritical region, the problem usually neglected in previous analyses. Its importance stems from the necessity of determination of the maximum possible area of wetted surface before the appearance of dry patches.

2. Stream spread on a horizontal surface

In general, stream spread on a horizontal surface, can be characterized by the presence of two zones: a zone of potential flow and a zone of viscous flow The region of viscous flow can be further divided into four characteristic sub-regions (see Fig. 1):

I. boundary layer region,

II. transition region,

III. hydraulic jump zone,

IV. subcritical region.

Fig. 1 presents also the extent of potential flow which can be divided into three more detailed sub-regions, as shown in [2]. Below, the problem of liquid stream spread in the subregions of viscous flow is only analysed.

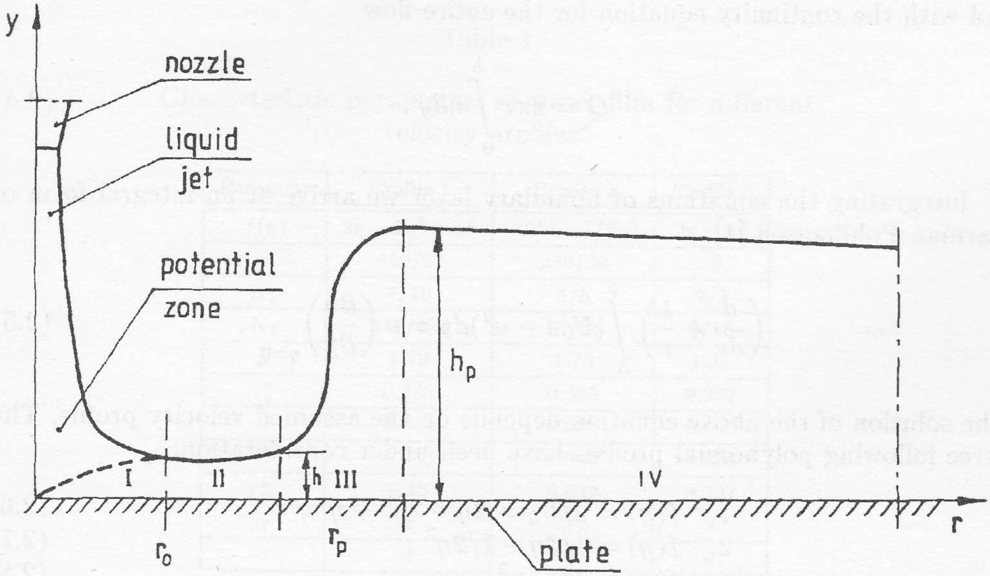

Fig. 1. Illustration of the jet impingement on a horizontal surface

Boundary layer region (I)

The region is characterized by the existence of both viscous and potential flow. The flow velocity varies from zero on the wall to a value of U_0 on the border of the boundary layer. The following assumptions are made in the analysis:

1. the flow of the liquid on the surface of the plate is stationary and laminar,
2. the liquid is considered to be incompressible,
3. the pressure gradient stemming from the mass and surface forces is negligible.

In accordance with the above assumptions the boundary layer equations take the following form:

$$u\frac{\partial u}{\partial r} + w\frac{\partial u}{\partial y} = \nu\frac{\partial^2 y}{\partial^2 y}, \tag{2.1}$$

$$\frac{\partial (ru)}{\partial r} + \frac{\partial (rw)}{\partial y} = 0\,, \tag{2.2}$$

with boundary conditions:

$$\begin{aligned} &\text{for} \quad y = 0, \quad u = w = 0\,, \\ &\text{for} \quad y = \delta, \quad \frac{\partial u}{\partial y} = 0\,, \end{aligned} \tag{2.3}$$

and with the continuity equation for the entire flow

$$Q = 2\pi r \int_0^h u dy \, . \tag{2.4}$$

Integrating the equations of boundary layer we arrive at an integral form of Karman-Pohlhausen [1]

$$\left(\frac{d}{dr} + \frac{1}{r}\right) \int_0^\delta (U_0 u - u^2) dy = \nu \left(\frac{\partial u}{\partial y}\right)_{y=0} \, . \tag{2.5}$$

The solution of the above equation depends on the assumed velocity profile. The three following polynomial profiles have been under consideration:

$$1. \quad f(\eta) = u/U_0 = 2\eta - 2\eta^3 + \eta^4 \, , \tag{2.6}$$
$$2. \quad f(\eta) = 3/2\eta - 1/2\eta^3 \, , \tag{2.7}$$
$$3. \quad f(\eta) = 2\eta - \eta^2 \, , \tag{2.8}$$

It can be shown that by assuming an appropriate profile in Eq. (2.5), a formula is obtained which describes the change of the boundary layer thickness in the considered region

$$\delta = \sqrt{\alpha \frac{\nu}{U_0} r} \, , \tag{2.9}$$

where: α is a coefficient dependent on the assumed velocity profile. Its values are given in Table 1. The liquid film thickness in the first region (I) can be determined with the aid of the continuity equation in the form:

$$Q = 2\pi r \int_0^\delta u dy + 2\pi r U_0 (h - \delta) \, . \tag{2.10}$$

Defining the quantities

$$\gamma = \left.\frac{df}{d\eta}\right|_{\eta=0} \, , \quad K_1 = \int_0^1 f(\eta) d\eta \, , \quad K_2 = \int_0^1 f^2(\eta) d\eta \, , \tag{2.11}$$

the liquid layer thickness is obtained from Eqs. (2.10) and (2.9)

$$h = \frac{Q}{2\pi r U_0} + (1 - K_1) \sqrt{\alpha \frac{\nu}{U_0} r} \, . \tag{2.12}$$

Bearing in mind that

$$Q = \pi a^2 U_0 \tag{2.13}$$

Table 1

Characteristic parameters of water film for different velocity profiles*

Parametr	Profile 1	Profile 2	Profile 3
$f(\eta)$	$2\eta - 2\eta^3 + \eta^4$	$3/2\eta - 1/2\eta^3$	$2\eta - \eta^2$
α	420/37	280/39	10
K_1	7/10	5/8	2/3
K_2	367/630	17/35	8/15
β	1.79	1.78	1.87
r_o^*	0.243	0.305	0.262
ω	0.642	0.685	0.656
Ω	5.033	4.042	5.236
r_m^*	0.40	0.439	0.397
γ	2	3/2	2
b	4	3	4

* They are defined in the text

and defining a non-dimensional radius r^* and the thickness h^* as:

$$r^* = \left(\frac{r}{a}\right) Re^{-1/3} , \tag{2.14}$$

$$h^* = \left(\frac{h}{a}\right) Re^{1/3} , \tag{2.15}$$

an expression is obtained from Eq. (2.12), which determines the change of the film thickness

$$h^* = \frac{1}{2r^*} + \beta\sqrt{r^*} , \tag{2.16}$$

where: $\beta = (1 - K_1)\sqrt{\pi\alpha}$. Values of coefficients K_1 i K_2 are given in Table 1. The radius r_0 where the boundary layer thickness coincides with the film thickness $(h = \delta)$ can be determined by the way of transformation of Eqs. (2.4), (2.9), (2.10) and (2.11) as

$$r_0^3 = \frac{1}{4\pi K_1^2\alpha}\frac{Qa^2}{\nu} , \tag{2.17}$$

or in the non-dimensional form as

$$(r_0^*)^3 = \frac{1}{4\pi K_1^2\alpha} . \tag{2.18}$$

Because for Profile 1: $K_1 = 0.7$, $\alpha = 420/37$ and for Profile 2: $K_2 = 0.625$, $\alpha = 280/39$, therefore the values of radius r_0^* vary between 0.242 and 0.305 for these selected velocity profiles. The third profile has values of K_1 and α similar to the first profile.

Transition region (II)

Within this region, the film thicknes coincides with the boundary layer thickness. In these circumstances it can be shown that by assuming a polynomial velocity profile like in the first region (I) velocity on the film surface and its thickness are given by the expressions:

$$U(r) = \frac{3K_2}{4\pi^2 K_1^2 \gamma} \frac{Q^2}{\nu(r^3 + l^3)}, \tag{2.19}$$

$$h(r) = \frac{2\pi K_1 \gamma}{3K_2} \frac{\nu(r^3 + l^3)}{rQ}, \tag{2.20}$$

where l is an integration constant determined from the conditions that for $r = r_0$, we have $U = U_0 = Q/\pi^2$

$$l = \left[\frac{1}{4\pi K_1^2}\left(\frac{3K_2}{\gamma} - \frac{1}{\alpha}\right)\frac{Qa^2}{\nu}\right]^{1/3} . \tag{2.21}$$

Placing the above into Eq. (2.20) we get the formula for the film thickness

$$h^* = \frac{\omega}{r^*} + \Omega(r^*)^2, \tag{2.22}$$

where:

$$\omega = \frac{1}{2K_1}\left(1 - \frac{\gamma}{3K_2\alpha}\right), \quad \Omega = \frac{2\pi K_1 \gamma}{K_2} . \tag{2.23}$$

For the selected velocity profiles values of the above coefficients are given in Table 1. The liquid film thickness in the region II has its minimum value for a radius r_m. This radius can be calulated from Eq. (2.22) by seeking roots of the first derivative. In the non-dimensional form r_m^* is equal to

$$r_m^* = \left(\frac{\omega}{2\Omega}\right)^{1/3} \tag{2.24}$$

For Profile 1, $r_m^* = 0.4$. For the remaining profiles values of r_m^* are given in Table 1.

Subcritical flow region (IV)

It extends beyond the region of hydraulic jump. The Froude number is less than unity in this case. Experimental investigations [2, 4] indicate that the film thickness varies unsignificantly, but is considerably higher than the thickness before the jump. In this region boundary conditions downstream of the jump seem to be of a major importance. The momentum and continuity equations for this region have the following form:

$$\frac{\partial (ru)}{\partial r} + \frac{\partial (rw)}{\partial y} = 0\,, \tag{2.25}$$

$$u\frac{\partial u}{\partial r} + w\frac{\partial u}{\partial y} = -\frac{1}{\rho}\frac{\partial p}{\partial r} + \nu\frac{\partial^2 u}{\partial y^2}\,, \tag{2.26}$$

$$-\frac{1}{\rho}\frac{\partial p}{\partial y} - g = 0\,, \tag{2.27}$$

with the boundary conditions:

$$\begin{aligned} &\text{at} \quad y=0, \quad u=w=0, \quad \partial u/\partial y = \tau_w/\rho, \\ &\text{at} \quad y=h, \quad \partial u/\partial y = 0, \quad \partial h/\partial r = w/u, \quad p = p_0\,. \end{aligned} \tag{2.28}$$

Because of the considerably greater film thickness than before, terms accounting for the pressure and gravity forces have been included in the momentum equations. It is convenient to present the continuity equation (2.25) in a slightly different form:

$$u\frac{\partial w}{\partial y} = -\frac{u}{r}\frac{\partial (ru)}{\partial r}\,. \tag{2.29}$$

Integrating Eqs. (2.29) and (2.26) over the film thickness we obtain:

$$uw\,|_0^h - \int_0^h w\frac{\partial u}{\partial y}dy = -\int_0^h \frac{u}{r}\frac{\partial (ru)}{\partial r}\,, \tag{2.30}$$

$$\int_0^h u\frac{\partial u}{\partial r}dy + \int_0^h w\frac{\partial u}{\partial y}dy = -\frac{1}{\rho}\int_0^h \frac{\partial p}{\partial r}dy + \nu\int_0^h \frac{\partial^2 u}{\partial y^2}dy\,. \tag{2.31}$$

From the boundary condition we have $uw\,|_0^h = U^2\dfrac{dh}{dr}$.
Because the integration limit h is variable, therefore the following relation has to be used:

$$\int_0^h u\frac{\partial u}{\partial r}dy = \frac{1}{2}\left[\frac{\partial}{\partial r}\int_0^h u^2 dy - U^2\frac{dh}{dr}\right] \tag{2.32}$$

where U is velocity in the r direction, for $y = h$. Two first integrals in Eq. (2.31) can be thus presented in the following manner:

$$\int_0^h u\frac{\partial u}{\partial r}dy + \int_0^h w\frac{\partial u}{\partial y}dy = \frac{d}{dr}\int_0^h \frac{u^2}{2}dy + \frac{1}{r^2}\frac{d}{dr}\int_0^h \frac{r^2u^2}{2}dy = \frac{1}{r}\frac{d}{dr}\int_0^h ru^2 dy\,. \tag{2.33}$$

Integration of the equation of motion (2.27) gives the pressure distribution over the film height

$$p = p_0 + gh(h - y), \tag{2.34}$$

hence,

$$-\frac{1}{\rho}\int_0^h \frac{\partial p}{\partial r} dy = -gh\frac{dh}{dr}. \tag{2.35}$$

The last viscous term in Eq. (2.31) can be transformed to

$$\nu\int_0^h \frac{\partial^2 u}{\partial y^2} dy = \nu\int_0^h \frac{\partial}{\partial y}\left(\frac{\partial u}{\partial y}\right) dy = -\frac{\tau_w}{\rho}. \tag{2.36}$$

Friction on the wall is expressed in terms of the friction coefficient C_f by the following relation

$$\tau_w = \frac{C_f}{2}\rho U^2, \tag{2.37}$$

therefore, the equation of motion (2.31) after utilizing the relations from (2.33) to (2.37) is brought into the form

$$\frac{1}{r}\frac{d}{dr}\int_0^h ru^2 + gh\frac{dh}{dr} = -\frac{C_f}{2}U^2. \tag{2.38}$$

Its solution depends on the assumed velocity profile. For the polynomial-type velocity profiles the obvious relations hold:

$$\frac{\bar{u}}{U} = K_1, \;\; K_1 = \int_0^1 f(\eta) d\eta. \tag{2.39}$$

Hence, taking into account the continuity equation

$$Q = 2\pi r h\bar{u} = const, \;\; \Rightarrow \;\; rh\bar{u} = const \tag{2.40}$$

the equation of motion in the radial direction is obtained from Eq. (2.38)

$$\frac{d}{dr}\left(\frac{U^2}{2}K_2 + gh\right) = -\frac{C_f}{2}\frac{U^2}{h}. \tag{2.41}$$

The friction coefficient C_f can be further expressed in terms of the Reynolds number in the following way

$$\tau_w = \mu\left(\frac{\partial u}{\partial y}\right)\bigg|_{y=0} = \mu\frac{U df}{h d\eta}\bigg|_{\eta=0}. \tag{2.42}$$

Combining Eqs. (2.42), (2.37) we obtain

$$C_f = \frac{b}{Re_h}, \tag{2.43}$$

where: $Re_h = \frac{hU}{\nu}$, $b = 2\gamma$.
By introducing the Froude number, the equation of motion (2.41) can be re-cast in the non-dimensional form as

$$(1 - K_2 Fr^2)\frac{dFr}{dR} = \frac{9}{32} b\, Fr^{11/3} - \frac{6Fr + 3K_2 Fr^3}{16R}, \tag{2.44}$$

where

$$R = \frac{r}{Re_h^{5/3} (\frac{\nu^2}{g})^{1/3}} \tag{2.45}$$

is a non-dimensional radius.
The last equation holds also for the transition region II, however, the influence of the gravitational force is there considerably smaller.

Hydraulic jump zone (III)

Hydraulic jump in the form of a sudden increase of the liquid film thickness is observed, when the flow is supercritical, i. e. when the Froude number is more than 1. After the hydraulic jump the flow is subcritical, i. e. $Fr < 1$. A simple analysis of this phenomenon can be conducted based on the conservation equations. Neglecting viscous terms, the change of momentum in the hydraulic jump region is compensated by the pressure increase. Therefore, the following relation holds [9]

$$\int_0^h u^2 dy - \int_0^{h_p} u^2 dy = \frac{1}{2} g (h_p^2 - h^2) \tag{2.46}$$

The radius r_p where the hydraulic jump occurs, is calculated based on the above relation assuming that $h \ll hp$ and additionally assuming a uniform velocity distribution after the hydraulic jump. The continuity equation may be then written as

$$Q = 2\pi r_p h U \int_0^1 f d\eta = 2\pi r_p h_p U_p . \tag{2.47}$$

Substituting Eq. (2.47) into (2.46) gives the jump radius

$$r_p = \frac{Q}{\sqrt{2g}\pi h_p} \sqrt{\frac{K_2}{K_1^2 h} - \frac{1}{h_p}} . \tag{2.48}$$

Investigations by Nakoryakov et al. [2] and Craik et al. [4] show that in the jump zone there are swirls and separation of the boundary layer. Under these circumstances taking into consideration the polynomial velocity profile instead of the uniform one seems to be justified. It can be shown that the radius r_p is then equal to

$$r_p = \frac{Q}{\sqrt{2g}\pi h_p}\sqrt{\frac{K_2}{K_1^2}\left(\frac{1}{h}-\frac{1}{h_p}\right)}\,. \tag{2.49}$$

In order to determine the jump radius from the above relation the film thickness h and h_p have to be known. The first quantity can be determined based on the relation (2.22). Whereas a priori determination of the second quantity h_p is difficult. Therefore, in practice various experimental correlations and additional assumptions are used. Steven and Webb [7] proposed for example the following correlation

$$r_p = 0.0061 d Re^{0.82}\,, \tag{2.50}$$

where: $Re = 4Q/\pi d\nu$. However, the authors of the paper [7] acknowledge that this correlation is far from accurate. The jump radius depends first of all on the thickness h_p after the jump. The latter in turn is influenced by the boundary conditions downstream of the jump. Olsson and Turkdogan [11] suggest that the position of the hydraulic jump should be determined from the relation

$$\frac{r_p}{a} Re^{-1/3} = 0.84 - 0.89\,. \tag{2.51}$$

On the other hand, Nakoryakov et al. [2] proposed that the jump radius should be calculated from the condition

$$\bar{u} = W\,, \tag{2.52}$$

where W is the velocity of disturbance propagation over the shallow water surface

$$W = \sqrt{gh}\,. \tag{2.53}$$

In other words this condition requires setting the Froude number $\bar{Fr} = 1$ for the jump. If values of U and h before the jump are known then the liquid layer thickness after the jump can be calculated from the balance of momentum (2.46) and the continuity equation. When the polynomial velocity profile is used before and after the jump, the ratio of the film thickness is expressed by

$$\frac{h_p}{h} = \frac{1}{2}\left(\sqrt{1+8K_2 Fr^2}-1\right)\,. \tag{2.54}$$

Relating the Froude number to the mean velocity we have

$$\frac{h_p}{h} = \frac{1}{2}\left(\sqrt{1+8\frac{K_2}{K_1^2}\bar{Fr}^2}-1\right)\,. \tag{2.54a}$$

For the polynomial velocity profiles the constant appearing in front of the Froude number is then about 9.6 whereas for the uniform distribution this coefficient is equal to 8.

Experimental investigations, for example in [4], [8, 9] show that contrary to shock waves in gases (an analogue of the hydraulic jump) the change of the liquid film thickness from h to a value of h_p takes place over a considerable distance reaching 20 mm and more depending on the Froude number before the jump. For the conditions when the plate is smooth and of dimensions 20 to 50 times greater than the nozzle diameter, then the jump takes place in the range of $\bar{Fr} = 2 \div 6$. Significant disturbances of the water surface are then also observed.

3. Experimental investigations

Experimental investigations of liquid spread on a horizontal plate caused by the impingment of a vertical jet was conducted on a special experimental arrangement depicted in Fig. 2. A pump was supplying water from the main tank to the

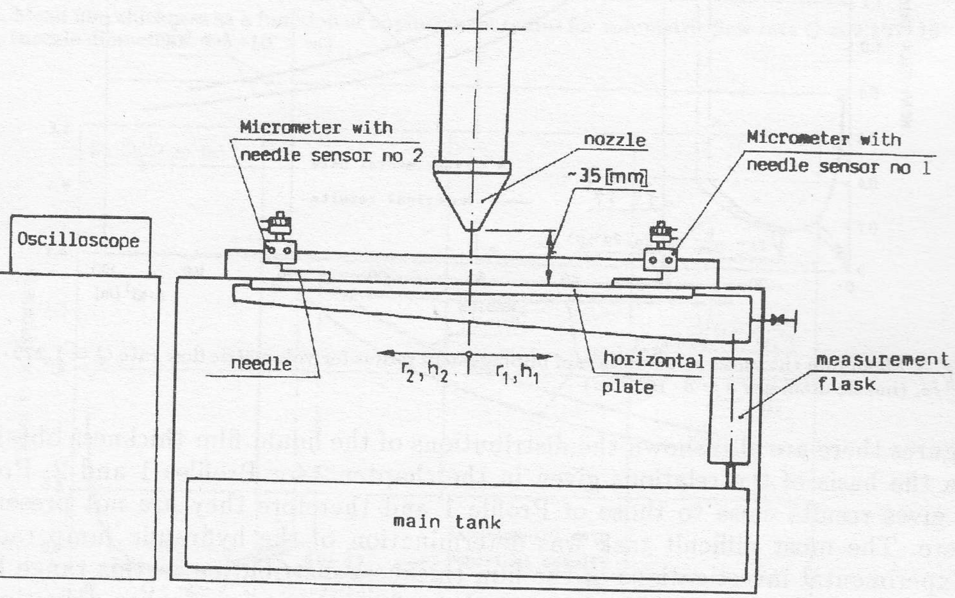

Fig. 2. Experimental arrangement

nozzle from where the liquid stream was impinging on the brass horizontal plate of dimensions 600 × 600 mm. The liquid film thickness was measured with the aid of a needle probe which utilized the change of resistance between the needle and the liquid layer. In order to avoid polarization of the electrodes, a probe (needle) was fed by altering voltage. A touch of the needle to the film surface closed the electrical circuit which could be observed in the change of the signal amplitude on the oscyloscope [10]. Two nozzles of diameters 3 and 5 mm were used in the investigations. Experiments were conducted in the flow range $Q = (1.16 \div 2.52)$ 10^{-5} m^3/s. The distance of the nozzle from the measurement surface was 35 mm in all experiments. All other details can be found in [11].

4. Discussion of results

Results of experimental investigations are presented in Figs. 3÷5. In the same

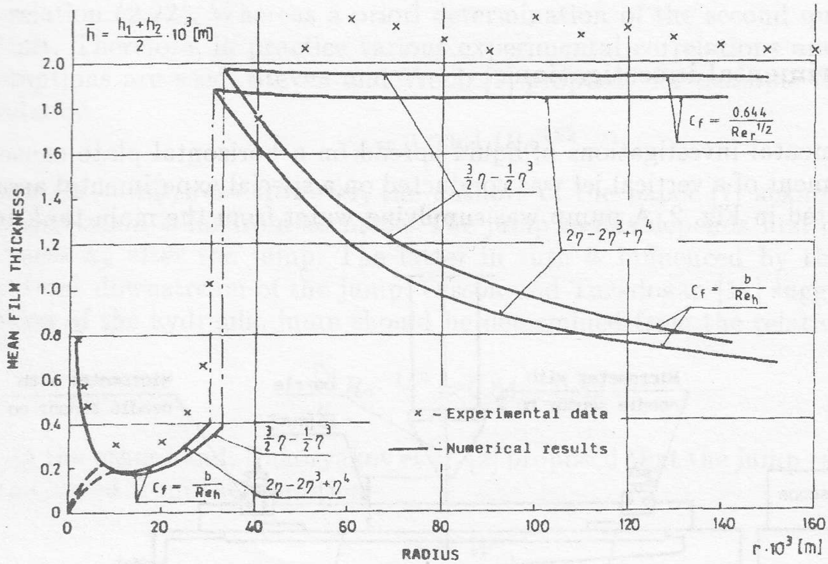

Fig. 3. Mean film thickness as a function of impingement radius for volumetric flow rate $Q = 1.222 \cdot 10^{-5}$ m^3/s, (nozzle diameter $d = 3 \cdot 10^{-3}$ m)

figures there are also shown the distributions of the liquid film thickness obtained on the basis of the relations given in the chapter 2 for Profiles 1 and 2. Profile 3 gives results close to those of Profile 1 and therefore they are not presented here. The most difficult task was determination of the hydraulic jump radius. Experimental investigations of the film thickness distribution in this range have shown that the length of the jump is about 20 mm. So far, precise definition of the jump radius has not been established. It may be sought, for example, as a radius of the beginning of the jump zone, the end of the zone, or the arithmetical mean of the two radii. This situation causes additonal discrepancies in results based on different definitions. In Table 2 there are presented values of the jump radius obtained by different authors. The values r_p given in the 1 and 2 rows were calculated assuming that the jump radius is determined by the locus where the film thickness is equal to $h_p/2$. The data given in the last row were obtained as singular points of Eq. (2.44). The left hand side of the equation is zero for

Table 2

Values of radius $r_p \cdot 10^3 m$

No.	The author	$Q[m^3/s]$	
		$1.22 \cdot 10^{-5}$	$2.52 \cdot 10^{-5}$
1	Craik et al. [4]	~ 31	51
2	Self investigations	30	53
3	Stevens and Webb [7], (2.50)	21.5	42.5
4	Nakaryakow et al. [2], (2.52)	27	43
5	Olsson and Turkdogan [12], (2.51)	25.5-27	46-49
6	Relation (4.1)	27-29	42-46

$Fr = 1/\sqrt{K_2}$. Comparing therefore the left hand side to zero, we obtain after transformation an expression for the jump radius

$$r_p = \left(\frac{2}{b\nu}\right)^{3/8} \left(\frac{K_2^4}{g}\right)^{1/8} \left(\frac{Q}{2\pi K_1}\right)^{5/8} . \tag{4.1}$$

Values of the jump radius given in Table 2 differ from each other significantly, especially for greater values of Q. Calculated values tend to be much lower than the experimental ones. However, even the experimental correlation of Stevens and Webb, Eq. (2.50), is not better than the approach of Nakoryakov et al. – Eq. (2.52) nor the relation (4.1). Distributions of the experimental data of the film thickness in the subcritical region are virtually uniform in the investigated range i.e. up to radius $r = 160\ mm$. Calculated values depend on the assumed formula for the friction coefficient C_f. Two calculating formulae have been taken into account for this range. The first one is based on the relation (2.43) and holds for the case where the boundary layer thickness is equal to the film thickness. The second approach is completely different. It is assumed there that immediately after the jump the boundary layer is formed and its thickness increases along the plate. In this case it is possible to use the Blasius formula to evaluate the friction coefficient in the same way as for the external flow over the plate. Then the friction coefficient is described as [13]

$$C_f = \frac{0.664}{Re_r^{1/2}} , \tag{4.2}$$

where: $Re_r = U(r - r_p)/\nu$

Results of calculations of the water film thickness presented in Figs 3÷5 together with the experimental data show that better consistency is achieved when relation (4.2) is used for the friction coefficient. Distribution of the film thickness is virtually flat in this case and differs by approximately 12 % from measured values and given in Figs. 3 and 5. The discrepancy is a little greater in the third case presented in Fig. 4. Some difficulties are encountered in determination of the film thickness due to the surface waviness. The point of contact of the needle with the surface is diffused. This is aggravated by the surface tension force which decreases or increases the liquid meniscus during the movement of the needle.

5. Conclusions

In the present work, the problem of radial liquid stream spread has been analysed both theoretically and experimentally. The influence of various velocity profiles on the film thickness has been analysed. For the supercritical region (before the hydraulic jump) the discrepancies between calculated and experimental values are not large. The differences are greater in the subcritical region (after the jump) and depend on the formula used for calculations of the friction coefficient. The biggest problem is, however, in determination of the hydraulic jump radius. None of the approaches existing in the literature returns satisfactory results. Therefore, it seems to be necessary to conduct further investigations in order to determine the position of the hydraulic jump and the parameters influencing it more precisely. When plates of large dimension are used, the behaviour of the liquid film is dependent on the surface condition like surface tension or wetting contact angle. The influence of the latter parameter has been least investigated so far.

Manuscript received December 19, 1994

References

[1] Watson E. J: *The radial spread of a liquid jet over a horizontal plane*, J. Fluid Mech. 20(1964), part. 3, 481÷499.

[2] Nakoryakov V. E., Pokusaev B. S., Troyan E. V: *Impingement of an axisymmtric liquid jet on a barrier*, Int J. Heat Mass Transfer. 21(1978), 1175÷1184.

[3] Rymkiewicz J., Trela M: *Zagadnienie rozpływu filmu cieczy przy prostopadłym napływie strugi na płaszczyznę poziomą*, Opracowanie IMP PAN, nr rej. 95/94, IMP PAN, Gdańsk 1994.

[4] Craik A. D, Lathan R. C., Jawkes M. J., Gribbon P. W: *The circular hydraulic jump*, J. Fluid Mech. 112(1981), 347÷362.

[5] Rahman M. M., Hankey W. L., Faghri A: *Analysis of the fluid flow and heat transfer in a thin liquid film in the presence and absence of gravity*, Int. J. Heat Mass Flow 34(1991), No. 1, 103÷114.

[6] Puzyrewski R., Sawicki J: *Podstawy mechaniki płynów i hydrauliki*, PWN, Warszawa 1987.

[7] Stevens J., Webb B. B: *Local heat transfer coefficients under axisymmetric, single-phase liquid jet*, Trans. ASME J. Heat Transfer 113(1991), 71÷78.

[8] Azuma T., Hoshino T: *The radial flow of a thin liquid film (2nd Report, liquid film thickness)*, Bull. of JSME, 27(1984), No. 234, 2747÷2754.

[9] Ishigai S., Nakanishi S., Mizuno M. Imomura T: *Heat transfer of the impinging round water jet in the interference zone of film flow along the wall*, Bull. of JSME, 20(1977), No. 139, 85÷92.

[10] Jaworek A: *Sonda igłowa do pomiaru grubości filmu cieczowego na stanowisku do badania kondensacji pary na warstwie cieczy*, Opracowanie IMP PAN, nr rej. 166/93, IMP PAN, Gdańsk 1993.

[11] Rymkiewicz J., Trela M., Ihnatowicz E: *Badania eksperymentalne struktur przepływu dla swobodnych strug cieczy na płaszczyźnie poziomej*, Opracowanie IMP PAN, nr rej. 174/94, IMP PAN, Gdańsk 1994.

[12] Olsson R. G., Turkdogan E. T: *Radial spread of a liquid stream on a horizontal plate*, Nature 211(5051), 1966, 813÷916.

[13] Kays W. M: *Convective heat and mass transfer*, McGraw-Hill, Inc. New York 1966.

Badania rozpływu cieczy przy napływie na poziomą płytę

Streszczenie

W pracy poddano analizie teoretycznej oraz badaniom eksperymentalnym rozpływ filmu cieczowego na poziomej płycie, powstały w wyniku pionowego napływu strugi. Przeanalizowano zmiany grubości filmu dla różnych obszarów przepływu, obejmujących również zjawisko uskoku hydraulicznego, przyjmując do obliczeń trzy różne profile prędkości. Szczególną uwagę zwrócono na zagadnienie lokalizacji uskoku hydraulicznego. Opisano stanowisko eksperymentalne, sposób pomiaru oraz przedstawiono wyniki badań. Wartości obliczeniowe grubości filmu dość dobrze zgadzają się z wartościami eksperymentalnymi.